Journal of Molecular Liquids 399 (2024) 124323

Contents lists available at ScienceDirect

Journal of Molecular Liquids

journal homepage: www.elsevier.com/locate/molliq

Surfactant-free oil-in-water nanoemulsions with nanopore membrane and ultrasound

Helena H.W.B. Hansen, Gregor Kijanka, Lingxi Ouyang, Nam-Trung Nguyen *, Hongjie An *

Queensland Micro and Nanotechnology Centre, Griffith University, 170 Kessels Road, Nathan, QLD 4111, Australia

ARTICLE INFO

Keywords:
Nanoemulsion
Stability
Surfactant-free
Dynamic light scattering
Nanoparticle tracking analysis

ABSTRACT

Hypothesis: Phase separation of heterogeneous liquids can occur in the presence of sufficient shear force between a solid interface and a liquid. We hypothesize that a continuous flow of oil through nanopores into water in combination with a given ultrasound energy can generate stable free standing oil emulsions in water in the absence of surfactants.

Experiment: An oil solution was pumped through a membrane with 100 nm pores at a controlled flow rate and introduced into an aqueous solution while being subjected to sonication. The resulting emulsion samples were collected at specific time intervals and characterized by dynamic light scattering and nanoparticle tracking analysis techniques. We evaluated the storage stability of the emulsions with and without surfactant at room temperature or 4 °C storage.

Results: Introducing oil into an aqueous phase using our Nanopore system in conjunction with ultrasound gave rise to surfactant-free milky oil nanodroplet solutions. Dynamic light scattering and nanoparticle tracking analysis showed that the produced surfactant-free oil nanodroplets were monodispersed in water at sizes less than 200 nm. Control experiments without the use of nanopores did not result in phase mixing. Nanoemulsions were also generated in a surfactant containing solution resulting in a similar size range of nanodroplets. This work demonstrates that our Nanopore system can generate stable nanoemulsions in the absence of a surfactant, persisting in phase separation for several days up to two weeks at room temperature and 4 °C storage. This work suggests that nanopores are effective in producing surfactant-free nanoemulsions, which offer a wide range of valuable applications varying from drug delivery and food engineering, to paints and pesticide development.

1. Introduction

Nanoemulsions are submicron droplets dispersed in another immiscible phase, traditionally generated using mechanical shear [1], with a wide range of applications in drug delivery [2], pharmaceuticals [3], cosmetics [3], food technology [4] and agriculture [5]. Emulsions are generally deemed unstable as liquids used for their creation are naturally immiscible and separate into their respective phases over time. The stability of nanoemulsions however, is superior owing to the nanometer size characteristics of the emulsion droplets. At this size range, emulsions can avoid aggregation and effects caused by gravity, such as separation [6]. Typically, the stability of nanoemulsions is further increased with the use of surfactants, which reduce the interfacial tension of the oil phase. Lowering the interfacial tension not only decreases the repellent nature of the two liquids, but also decreases the attraction between the oil droplets [1]. In addition to increased stability, nanoemulsions exhibit increased bioavailability, enhanced absorption, and a high surface area to volume ratio [2]. These characteristics make nanoemulsions uniquely functional for medical applications such as drug delivery.

In healthcare, a variety of natural oils are used for nanoemulsion formulation including eucalyptus [7,8], palm oil [5], virgin coconut oil [9], rapeseed oil [10], and sesame oil [11]. In combination with a drug, nanoemulsions often show a synergistic effect, permitting the same level of treatment at a significantly lower drug dosage. Regulatory approved medicines that have been combined with oil emulsions include, but are not limited to, cholesterol lowering atorvastatin [12], anticancer curcumin [13] and doxorubicin [7], and a range of vitamins [14]. All these drugs have one essential similarity: they're hydrophobic. Administration of these drugs using conventional methods is difficult as dosage and bioavailability present an issue. However, both can be overcome by dissolving the otherwise insoluble drug in oil, and delivering it as an emulsion.

* Corresponding authors.
E-mail addresses: nam-trung.nguyen@griffith.edu.au (N.-T. Nguyen), hongjie.an@griffith.edu.au (H. An).

https://doi.org/10.1016/j.molliq.2024.124323
Received 30 November 2023; Received in revised form 16 February 2024; Accepted 22 February 2024
Available online 28 February 2024

A major drawback of traditional emulsions is that they are often cumbersome to generate. In addition, production processes often require the addition of surfactants, which may lead to adverse health effects in patients, depending on the exposure levels. The effective generation of stable nanoemulsions is a non-trivial task and it has been the focus of a wide range of advancement attempts. Popular generation methods include dedicated homogenizers [10], microfluidics [15], phase inversion [14], freeze drying [16], solvent evaporation displacement [17] and stirring [18], which are typically technically demanding, requiring several days to complete. In addition, the steps involved may result in the degradation of the active ingredients or loss of sub-micron materials. Furthermore, compared to other dosage formulations, they are often quite unstable as consequence of Oswald ripening resulting in a shortened shelf life [1]. Bypassing such hurdles often necessitates the addition of surfactants. Common surfactants include Tween 20 and Span 80, [19], egg yolk powder [13] and soybean protein isolate [16]. Traces of other undesired chemicals may be found in the surfactant solutions deriving form production processes, which may include, but are not limited to, ethyl alcohol [16] and petroleum ether [19]. Although effective in stabilizing oil emulsion formulations, traces of surfactants may lead to unwanted side effects when used in humans, resulting in significant post-processing challenges. Studies investigating surfactant use in nano formulations have shown considerable side effects, highlighting the importance of surfactant choice and concentration [20,21]. A complete absence of surfactants during nanoemulsion production processes for pharmaceutical formulations is ideal, helping to avoid patient exposure to traces of contaminants, while, at the same time, significantly reducing production costs.

This paper introduces a simple, surfactant-free approach for nanoemulsion generation that delivers stable nanoemulsions in aqueous solutions, thereby circumventing many of the issues associated with traditional emulsion generation and surfactant use. Herein, we aim to generate a nanoemulsion using a nanopore membrane in combination with sonication. We hypothesize that a liquid passing through a nanopore that is introduced to a non-miscible liquid can be broken down with a shearing force provided, for example, by ultrasound.

We conducted a thorough characterization and stability analysis of the resulting nanoemulsions, and we demonstrate the stability of our surfactant-free oil nanoemulsion synthesized in water at physiological pH. In this study we considered the effects of storage time and temperature, as well as the impact of surfactant additives on generated nanoemulsions. Moreover, we successfully incorporated the well-known cancer drug curcumin into the nanoemulsion formulation to demonstrate potential applications of nanoemulsions as a carrier in drug delivery.

2. Materials and methods

2.1. Materials

Sodium dodecyl sulfate (SDS), Triton X, phosphate buffered saline (PBS), and curcumin were purchased from Sigma Life Sciences. 0.02-μm and 0.45-μm syringe filters were purchased from Whatman and Millex®, respectively.

The Nanopore system was constructed using transparent tubing, glass Pasteur Pipets, 0.1 μm PC Membrane (Isopore^{TM}, Thermo Fisher Scientific), and epoxy glue (Shellys® Araldite 5 min epoxy adhesive). The oil solution was introduced by way of a syringe pump (Adelab Scientific), in conjunction with an VEVOR® Digital Ultrasound Cleaner.

2.2. Solution preparation

Curcumin from Sigma Aldrich was dissolved in sunflower oil to a concentration of 0.5 mg/mL. The solution was brought to 90 °C in a water bath for two hours under constant stirring till the curcumin powder had been dissolved. A 5 mM SDS solution was prepared using MilliQ deionized (DI) water at a pH of 7.4. Before introduction of oil, DI water and 5 mM SDS were filtered using a 0.02-μm filter. One day before emulsion generation, aliquots of DI and 5 mM SDS were placed at 4 °C.

2.3. Scanning electron microscopy

The Isopore filters were imaged using scanning electron microscopy (SEM). The filter was cut into small pieces and fixed on the SEM sample holder and sputter coated with a 10 nm thick platinum layer before imaging. The treated samples were characterized with the JEOL JSM 7100F SEM under an accelerating voltage of 10–15 kV.

2.4. Characterization

Dynamic light scattering (DLS, LiteSizer 500, Anton Paar) was used to evaluate size distribution of prepared oil in water nanoemulsions. The DLS measurements allowed us to assess the stability of the samples. As DLS does not consume the sample, a set of measurements was completed using a single aliquot of the generated emulsion kept in one cuvette. This protocol enhances the sensitivity by avoiding errors introduced by factors such as nonuniform mixing, flow rate, environmental noise while changing samples, etc. However, DLS failed to measure the concentration of the nanoemulsions. Concentration was therefore characterized using the nanoparticle tracking analysis (NTA) system NanoSight NS300 (Malvern Panalytical), concurrently collecting data on particle size and size distribution. However, stability measurements using NTA were not possible using a single sample volume due to sample losses amid passing through the visualizing window in course of the measurements. As such a new aliquot of the generated emulsion was extracted for each measurement. The NanoSight was cleaned with a washing buffer containing 2 % Triton X in PBS at pH 7.4 between all measurement. The system was rinsed with DI water before and after use of the washing buffer. Ten measurements of 15 s each were taken for each sample volume. As the NTA provides concentration measurements in the unit of particles per milliliter, the oil droplets that make up the emulsion will be referred to as particles.

For stability studies, measurements were carried out at different time stamps after generation for insight into their dynamic changes with regards to concentration and size. The timing was set up from 0 h up to 2 weeks with the following measurement points: 0 h (time of generation), 1 h, 6 h, one day (24 h), two days (48 h), one week (168 h), and two weeks (336 h) after generation. The samples were diluted 1:4 in accordance to NanoSight manufacturer recommendations to ensure an appropriate particle concentration. This concentration was kept consistent for all measurements. As the NanoSight computed a data set in a range up to 1 μm, we also used DLS to analyze samples in ranges up to 10 μm.

2.5. Curcumin concentration

Curcumin encapsulation was measured using ultraviolet–visible spectroscopy (SP-8001 UV–Vis, Taiwan) in oil emulsions without curcumin (sunflower oil emulsion) as control. A calibration curve was generated using concentrations from 1 to10 μg/mL. The stock solution was diluted a factor of ten times and used for generation of further diluted samples. Each sample was measured ten times, and the mean value was calculated for each concentration. The data was fitted with linear regression. Pure sunflower oil was used as background control for generation of the calibration curve and was subtracted during the measurements. The absorption was measured at a wavelength of 425 nm; the absorption peak for our oil/curcumin solution. To confirm the presence of curcumin in the oil emulsions, representative samples were generated with an oil emulsion without dissolved curcumin acting as the baseline. The baseline was subtracted from the curcumin containing emulsions during the measurements.

2.6. Statistics

All data are represented as the mean size for at least three independent experiments. One-way analysis of variance (ANOVA) was used to determine statistical significance between the groups, here presence of a surfactant, and storage temperature. In all cases p-values < 0.05 were taken as statistically significant and p-values < 0.01 were taken as very statistically significant.

3. Results

3.1. Nanopore system and experimental setup

The Nanopore system (Fig. 1a) was built using plastic tubing with a glass Pasteur pipette inserted into the tubing to increase the rigidity of the system. The 0.1 μm membrane filter was attached to one end of the system, with all parts sealed with epoxy glue. The size of the nanopores was characterized by SEM (Fig. 1a insert) to verify the pore sizes. The SEM image showed uniform pores with a size of 108 ± 3.5 nm. This is consistent with its nominal size provided by the manufacturer. A syringe containing the oil/curcumin solution was attached to the syringe pump to control the flow rates at which the oil solution was pumped through the membrane and introduced to the aqueous phase (Fig. 1b).

The membrane was placed in contact with the aqueous solution: either DI water or 5 mM SDS. This process was carried out with care to remove all air present in the system. The set flow rate was 5 μL/min, and the sonication time was 10 min at fixed frequency of 20 kHz and input power 150 W. The pump and the ultrasound bath were started and stopped simultaneously. The resulting samples were lightly opaque in appearance due to the generated emulsion. After the generation process, the samples were either stored at room temperature or at 4 ℃ according to the initial storage condition of the aqueous phase. All samples were purified with a 440-nm filter before characterization to remove any possible large oil droplets introduced during the removal of the nanopore system from the sample. Four samples were generated in total: surfactant-free oil emulsions stored at room temperature or at 4 °C (cold storage), and surfactant oil emulsions stored at room temperature, or at 4 °C.

3.2. Emulsion generation

To verify our assumption that the Nanopore system is necessary for proper generation of oil emulsions, we introduced the oil/curcumin solution in DI water without using nanopores and then sonicated for 10 min. As expected, no mixing occurs (Fig. 2b). This clearly shows that the oil and water phases stay within each compartment phase with a clear interface. In contrast, the samples using nanopores resulted in milky white solutions as shown in Fig. 2c. The concentration of the oil emulsion is proportional to the sample generation time.

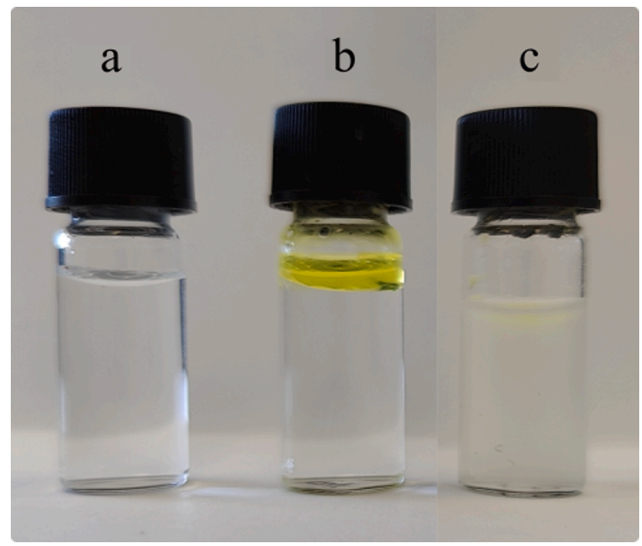

Fig. 2. Photos of nanoemulsions generated in DI water. a) negative control, sample containing only DI water, b) control without using Nanopore system, sample with curcumin oil solution added directly to the vial and sonicated for 10 min and c) curcumin oil emulsion generated using the Nanopore system with a flow rate of 5 μL/min for 10 min while placed in an ultrasound bath.

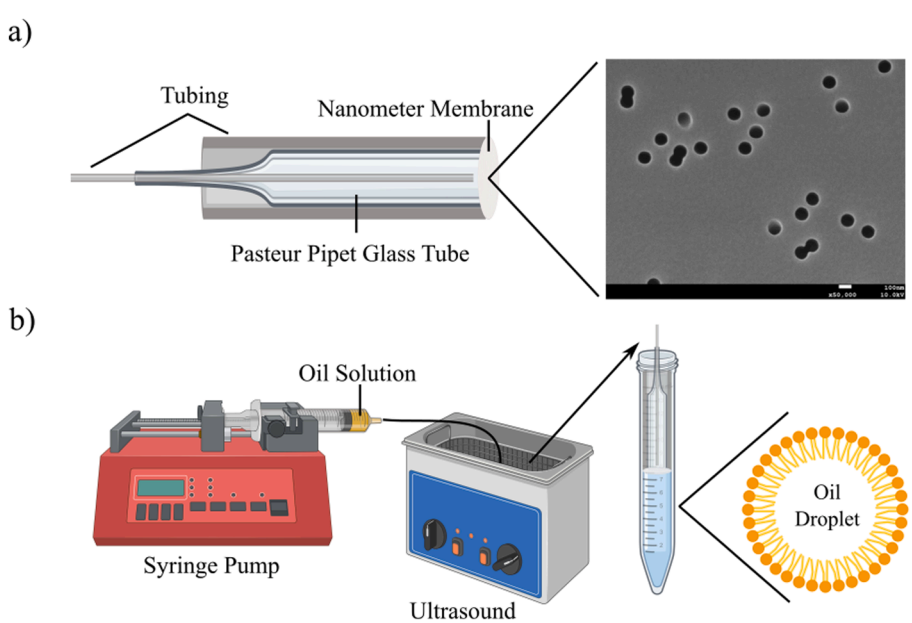

Fig. 1. A) schematic setup of nanopore system. the insert shows a SEM image of the 100 nm membrane filter. The scale bar is 100 nm. b) Schematic of setup for oil emulsion generation using ultrasound. A syringe containing the curcumin/oil solution is attached to a syringe pump. Tubing connects the syringe to the vial containing the aqueous solution which is placed in an ultrasound bath. The resulting solution contains oil micelles with encapsulated curcumin. Created with BioRender.com.

3.3. Emulsion size distribution via DLS

The size distribution of oil droplets in water was first characterized by DLS (Fig. 3). To study the stability of the emulsion over time the size and particle concentration was measured over a period of two weeks at the following times: 0 h (at time of generation), 1 h, 6 h, 24 h (1 day), 48 h (2 days), 168 h (1 week), and 336 h (2 weeks) after generation.

The DLS data shows one peak in the range up to 10 μm with a polydispersity index between 0.12 ~ 0.18 for all four samples, indicating the droplets are monodispersed. The surfactant-free samples at room temperature (Fig. 3a) at 0 h has a peak at 188 nm, with an average size of 190.8 ± 4.1 nm. There is no visible change in the first hour after generation. This sample was stable in the following 14 days having a peak at 188 nm after two weeks with an average size of 191.4 ± 4.4 nm. The minimal change in size distribution over the measurement period is indicative of a very stable nanoemulsion.

The surfactant-free sample stored at 4 °C (Fig. 3b) did not experience obvious changes over the course of two weeks. There are no notable changes in the first 6 h, both in size and percentage of intensity. The only observation was a slight change in size, with a shift from 188 nm to 204 nm, with the mean size starting at 208.5 ± 1.0 nm, and increasing to 219.4 ± 4.6 nm, after the first 6 h. The shift of 20 nm is negligible when taking into consideration the method of measurement. Therefore, the cold storage surfactant-free sample was relatively stable but showed a small dynamic change with respect to its storage conditions.

To illustrate the efficacy of our method, we compared our surfactant-free emulsions to similar emulsions generated in an aqueous phase containing a surfactant, here SDS. The concentration of SDS is set to 5 mM which is below its critical micelle concentration of 8 mM [22]. The surfactant emulsions were characterized using DLS with the same protocol as for surfactant-free emulsions. The DLS results of the surfactant sample stored at room temperature, and its stability at different times after generation can be seen in Fig. 3c. Like the surfactant-free samples, one peak was observed in the range up to 10 μm, suggesting a monodispersed emulsion. It has a peak at 188 nm at 0 h, with an average of 209.2 ± 2.9 nm. The size for this sample remained constant over the two-week measurement period with the average size decreasing slightly to 199.7 ± 1.3 nm. However, the percentage of intensity decreased over time from ca. 11 % to 9 %.

Similarly, the surfactant sample stored at 4 °C (Fig. 3d) showed a single peak, with no extreme changes over the course of two weeks. The mean size of the cold storage sample increased from 174 nm to 204 nm within the first 24 h after which it remained relatively stable at 209 ± 1.0 nm. The percentage of intensity also reduced at the peak size. As with the other samples the DLS data suggests a dynamic change in intensity rather than size, of the cold storage surfactant sample.

3.4. Nanoemulsion size distribution and concentration via NTA

NTA was used to analyze our four samples to obtain more detailed information regarding particle size and concentration. Like DLS, NTA also provides a size distribution peak. However, NTA data is based on the measurements of individual particles in the sample rather than a mean of the whole sample thus providing more detailed information on the size as well the concentration distribution of the nanoemulsions. As NTA measurements consume the samples, it was not possible to use the same volume for each measurement. Therefore, each measurement was done using a new aliquot of the original emulsion.

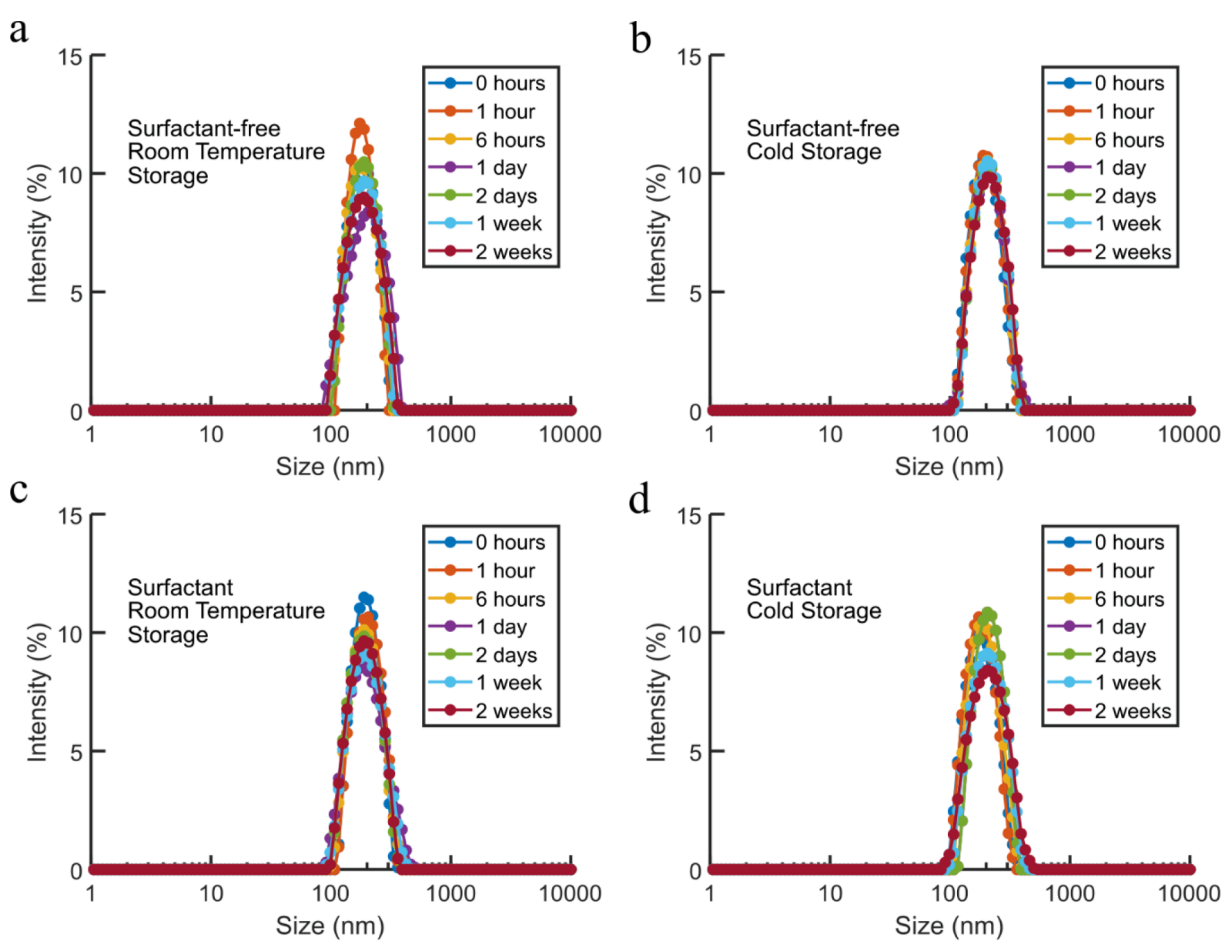

Fig. 3. Size distribution of the nanodroplets obtained with LiteSizer for surfactant-free oil/curcumin emulsion stored at (a) room temperature and (b) 4 °C, and surfactant oil/curcumin emulsion stored at (c) room temperature and (d) at 4 °C over a period of two weeks.

Fig. 4a and 4b present the NTA data for the room temperature storage surfactant-free sample. At 0 h, the dominant peak is observed a concentration of 3.23 × 10^7 particles/mL. The total particle concentration at this time was 1.78 × 10^9 particles/mL. Over the next 6 h the peak concentration increased to 5.78 × 10^7 particles/mL. The dominant peak reached a maximum concentration at 24 h with 6.11 × 10^7 particles/mL after which the concentration decreased. After two weeks the peak concentration for the room temperature surfactant-free sample was 3.79 × 10^7 particles/mL, and the total particle concentration was 1.64 × 10^9 particles/mL. The peak had a marginal shift with regards to particle size but doubled within the first 48 h with respect to particle concentration only to decrease again.

For storage at 4 °C, the surfactant-free emulsion (Fig. 4c and 4d) showed an initial peak concentration of 6.66 × 10^7 particles/mL. In contrast to its room temperature counterpart, this peak increases steadily over time to 8.22 × 10^7 particles/mL at the two-week mark. The total particle concentration of the cold storage surfactant-free sample at 0 h was 3.81 × 10^9 particles/mL and increased to 3.95 × 10^9 particles/mL after two weeks. Comparing Fig. 4c and 4d we observed that over time the particle size distribution shifted slightly to the left, with the peaks at 200 nm disappearing. This indicates a good stability and a small polydispersity in our sample. An interesting observation was the large increase in particle concentration when comparing this sample to its room temperature counterpart.

At 0 h (Fig. 5a and 5b) the room temperature surfactant emulsion presented with a peak concentration of 3.38 × 10^7 particles/mL. The total particle concentration at 0 h was 1.86 × 10^9 particles/mL. After one week the concentration of the dominant peak increased to 5.60 × 10^7 particles/mL, only to decrease to 4.44 × 10^7 particles/mL at the two-week mark. At this time the total particle concentration was 2.2 × 10^9 particles/mL. When comparing Fig. 5a and 5b we see that, besides the dominant peak, there are multiple smaller peaks at larger particle sizes. These peaks are still present after two weeks, suggesting that there is a gradual change in size over time, but overall, the emulsions are stable during long-term storage.

The last sample, cold storage surfactant emulsion, (Fig. 5c and 5d) presented with a dominant peak with a concentration of 6.33 × 10^7 particles/mL at 0 h. The total concentration at this time was 3.35 × 10^9 particles/mL. Within the first hour this peak decreased to 3.64 × 10^7 particles/mL and increased to 9.57 × 10^7 particles/mL after 6 h. After 48 h the mode concentration decreased again to 6.23 × 10^7 particles/mL but increased back to 9.98 × 10^7 particles/mL at two weeks. The final total particle concentration of the sample was 4.19 × 10^9 particles/mL. Even though the particle size remained relatively constant over time, the concentration showed a tendency to shift dramatically. This may be a combined issue when taking into consideration the storage and measurement temperatures along with the presence of a surfactant.

From the NTA data it was observed that the particle concentration for all the samples had a marginal increase over the two-week measurement period with respect to their initial concentration. The size distribution showed more change over time shifting to smaller sizes while decreasing in concentration with respect to particles larger than 100 nm,

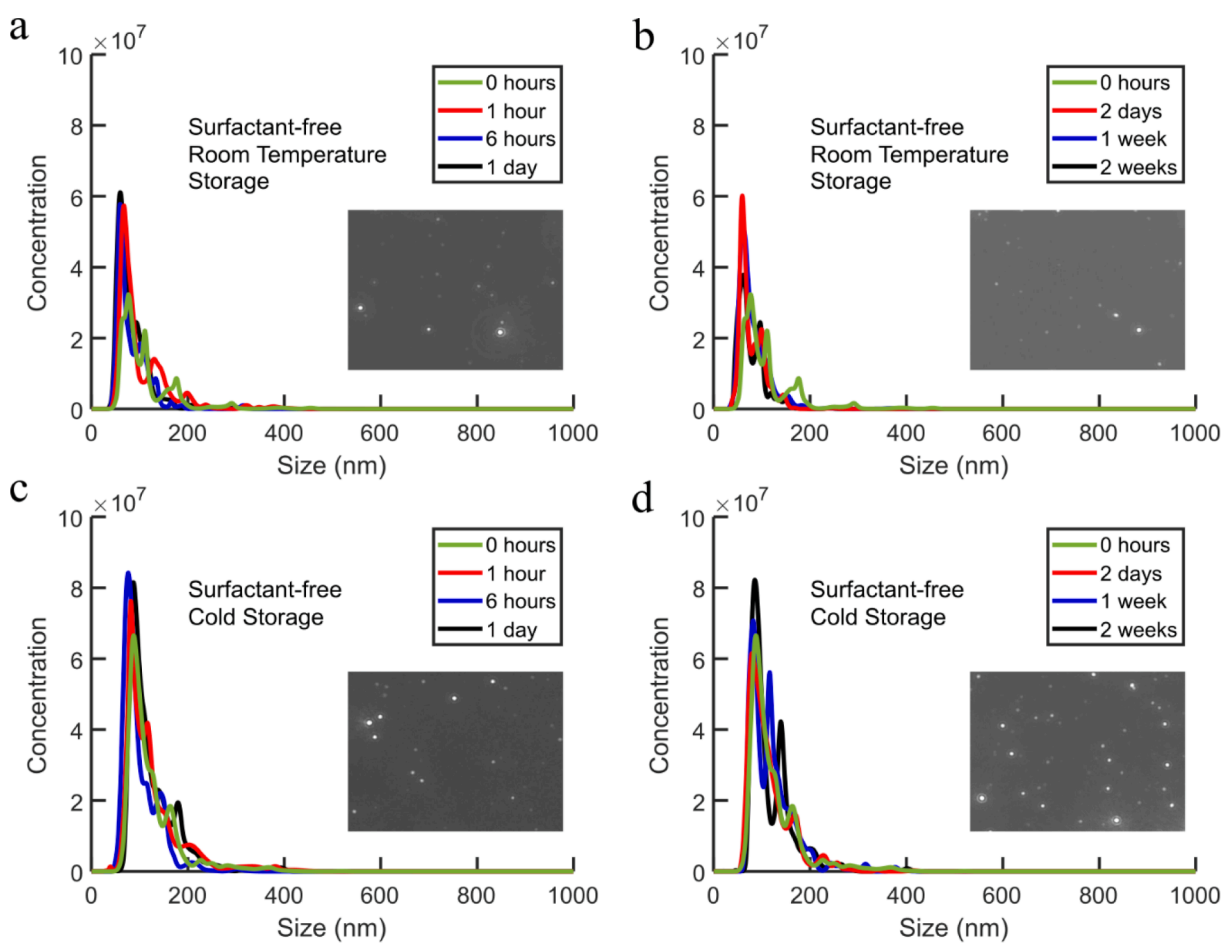

Fig. 4. Concentration distribution of surfactant-free emulsions measured by NTA. Samples stored at room temperature (top row) and at 4 °C (bottom row). The concentration unit is particles/mL. Inserts are representative images of NTA image files at 0 h, and 2 weeks respectively from left to right.

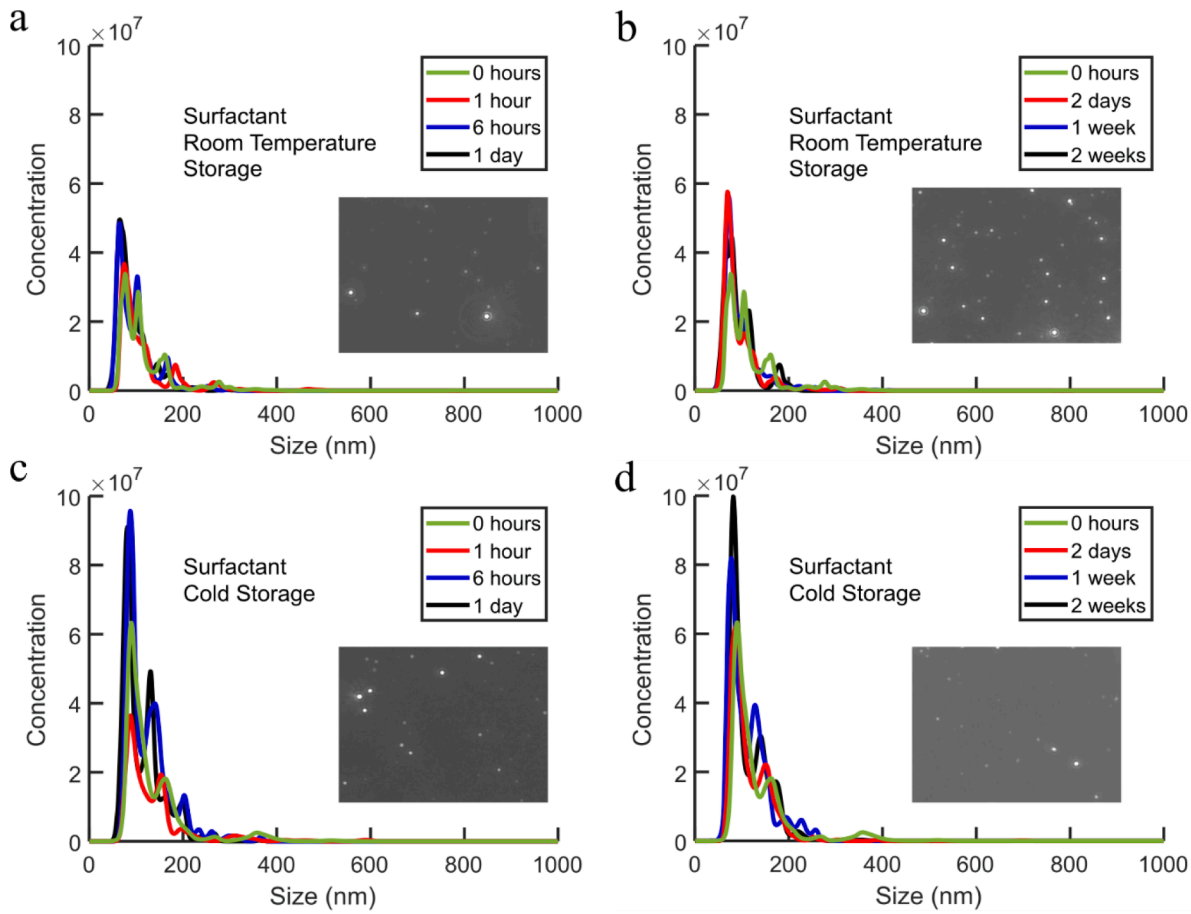

Fig. 5. Concentration distribution of surfactant emulsions measured by NTA, with the unit particles/mL. Samples stored at room temperature (top row) and at 4 °C (bottom row). Inserts are representative images of NTA image files at 0 h, and 2 weeks respectively from left to right.

3.5. Sample comparison

Fig. 6 summarizes the size and total concentration of surfactant-free and surfactant samples during storage at room temperature or 4 °C. From Fig. 6a we see that over the first six hours the surfactant-free sample (blue) decreases in size after which it stabilizes, compared to the surfactant sample (red) which maintains it size over the two-week measurement period, albeit with a small downward trend. For the cold storage samples (Fig. 6c) we observed a more stable emulsion with respect to size. Comparing the sizes of the surfactant-free and surfactant samples at room temperature and cold storage, we find that there was no difference for the surfactant sample at either storage temperatures ($p = 0.89$), whereas a very significant difference was observed ($p = 0.0001$) for the surfactant-free sample.

Fig. 6b and 6d show the overall concentrations for the samples at room temperature and cold storage respectively, given by NTA. The initial sample concentration for the cold storage samples (Fig. 6d) was twice that of the room temperature samples (Fig. 6c) and remained so throughout the stability study. For the surfactant sample in cold storage the particle concentration jumps several times during the first 6 h. This may be due to the temperature change that occurs during measurement as all NTA measurements were performed at 25 °C. One possibility for the fluctuation is the nucleation of nanosized air bubbles due to the temperature change. Henry's law states that as the temperature increases the solubility of gas decreases. This means that in our cold storage samples there is a higher likelihood of gas nanobubble generation as more air can be dissolved within the system. These bubbles may form as the sample is heated during the measurement, interacting with the oil emulsion, and possibly blocking their presence from the system by generating larger particles. As a new aliquot was taken for each measurement, the gas would slowly seep out of the emulsion giving us a more stable sample in the later measurements. The particle concentration in all samples varied over time but remained relatively stable compared to the initial concentration. For both the surfactant-free and surfactant samples there was a significant difference ($p < 0.0001$, and $p = 0.0004$ respectively) between the storage temperatures.

4. Discussion

4.1. Oil emulsion generation

The generation of emulsions in this study required careful positioning of the filter with respect to the water level in the ultrasound bath so the oil wasn't affected by the ultrasound before passing through the filter. The produced surfactant-free oil emulsions in water (Fig. 2) clearly support our initial hypothesis that adding oil to an aqueous solution followed by ultrasonication does not result in a nanoemulsion. Rather, passing the oil through a filter in combination with ultrasound, is a vital step in nanoemulsion generation. However, several critical factors need to be considered while processing emulsions, including the impact of fabrication conditions such as flow rates and energy effects of the ultrasound, storage temperature, long-term stability, and drug encapsulation. In initial experiments we tested the effects of the initial nanoemulsion size with respect to pump speed and ultrasound time. We found that a pump speed of 5 μL/min resulted in the most stable emulsions with the desired emulsion size. In addition, the ratio of introduced oil volume to total sample volume played a major role in how the size and concentration of oil droplets changed over time. Excessive

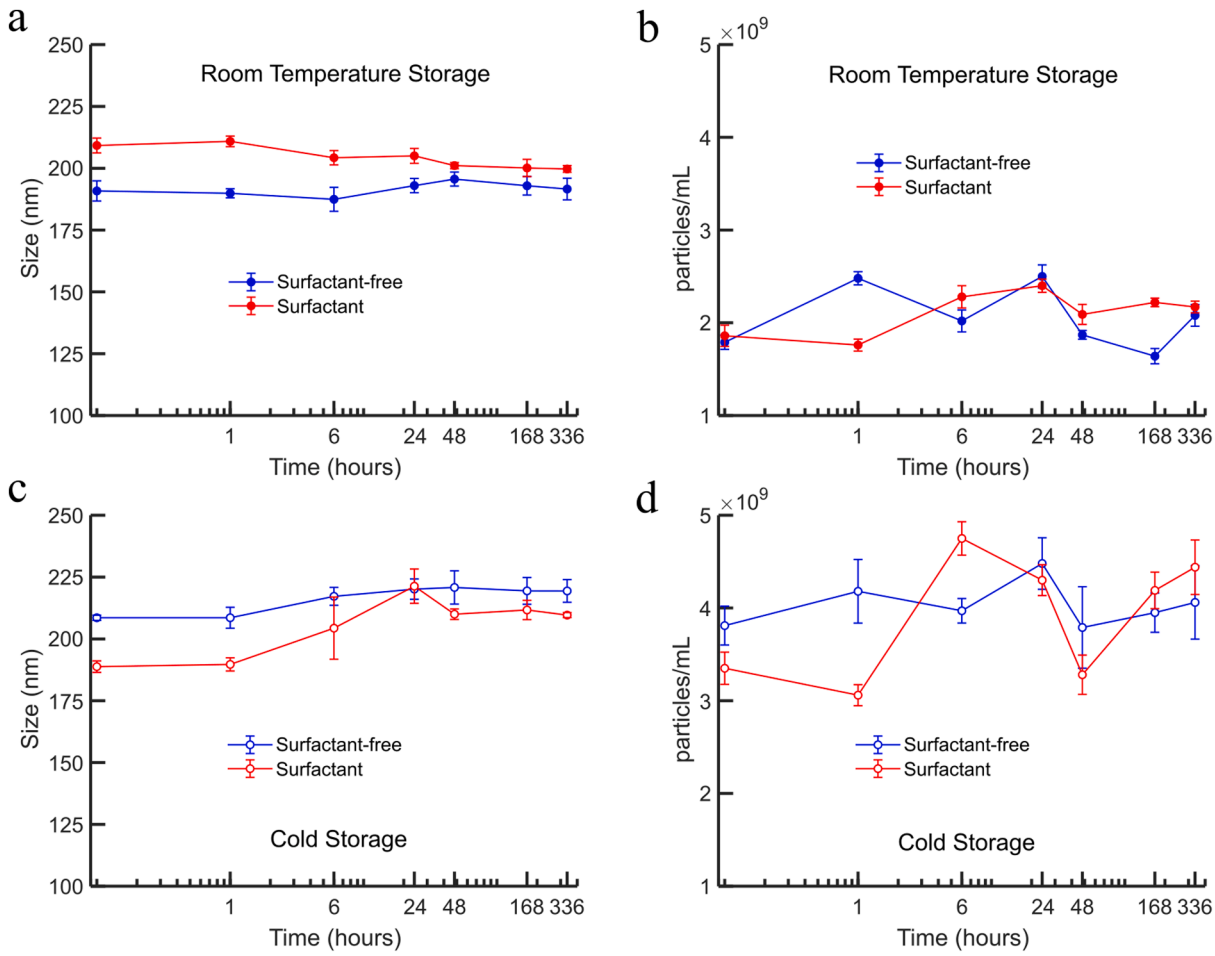

Fig. 6. Change in size and concentration for room temperature (a and b respectively) and cold storage (c and d respectively) samples. Blue: surfactant-free samples, red: surfactant samples. Measurements taken at: 0 h (at time of generation), 1 h, 6 h, 24 h (1 day), 48 h (2 days), 168 h (1 week), and 336 h (2 weeks) after generation. (For interpretation of the references to color in this figure legend, the reader is referred to the web version of this article.)

oil volumes introduced into water repeatedly lead to large quantities of oil nanodroplets appearing as a dense emulsion cloud, thus effecting particle stability due to Brownian motion-initiated collisions and dynamic change due to Ostwald ripening. At longer generation times, droplet size would change drastically over time. We also tested the influence of ultrasound power on particle size distribution, finding little impact at 30 W and 150 W set ultrasound.

During generation, no entrapped air could be within the Nanopore system or the sample tube. Trapped air can facilitate cavitation or act as cavitation nuclei, effectively changing the characteristics of the emulsions as well as introducing nanobubbles that would be picked up by the NTA without means for distinguishing them from the oil droplets during the measurements. In addition, ultrasound induced cavitation will damage the adjacent wall [23–25], the nanopore membrane in this case. Breakdown of the membrane would generate coarse droplets resulting in a solution with a high polydispersity. An intact nanopore filter is necessary for successful generation of nano-emulsions as seen in Fig. 2.

4.2. Stability

We have demonstrated that surfactant-free nanoemulsion produced with our approach display highly stable characteristics regardless of storage conditions. Excellent emulsion stability opens a wide world of potential applications. So, what stabilizes the oil droplets in water? Understanding the attributes enabling oil droplet stability in immiscible liquids have exhibited significant scientific interest from both, the fundamental and applied perspectives. The historical interest of oil suspension in water originates from the discovery of the “ouzo effect”, the spontaneous emulsion effect, which occurs when ethanol containing essential oil meets with water [26]. Even though this is a decades old discussion, it is no less mysterious with years of research dedicated to understanding this effect.

Several possible factors have been attributed to the stability of oil in water or water in oil droplet over the years. In many cases, the emulsions surface charge is thought to play an important role in stabilizing colloidal particles [27–29]. However, in this study, the zeta potential of surfactant-free oil in water emulsion was measured at 2.22 mV (Fig. 7a) and 1.65 mV for the surfactant sample (Fig. 7b). With a charge that close to neutral, surface charges are less likely to be responsible for stabilization of surfactant-free emulsions in this study. Several other studies proposed that the formation of hydrogen bonds at the interfaces between water and oil stabilizes the droplets [30].

A study by Carpenter *et al.* [31] generated low-charge stable bare emulsions using ultrasound which had near zero surface charge. Using surface spectroscopy, the authors found free OH vibrations attributed to stronger dispersal interactions. Moreover, addition of an anionic surfactant reversed these vibrations. Addition of anionic surfactants (like SDS used in our experiments) have a negative charge resulting in the disappearance of the observed OH vibrations. The authors discuss that this may interfere with dispersion forces between droplets, thus impacting the overall stability. In the absence of a surfactant, the system can stabilize itself with respect to the aqueous solution, as there are no additional factors effecting the hydrogen and hydroxide bonds present at interface. The dispersal interactions displayed by free bonds at the

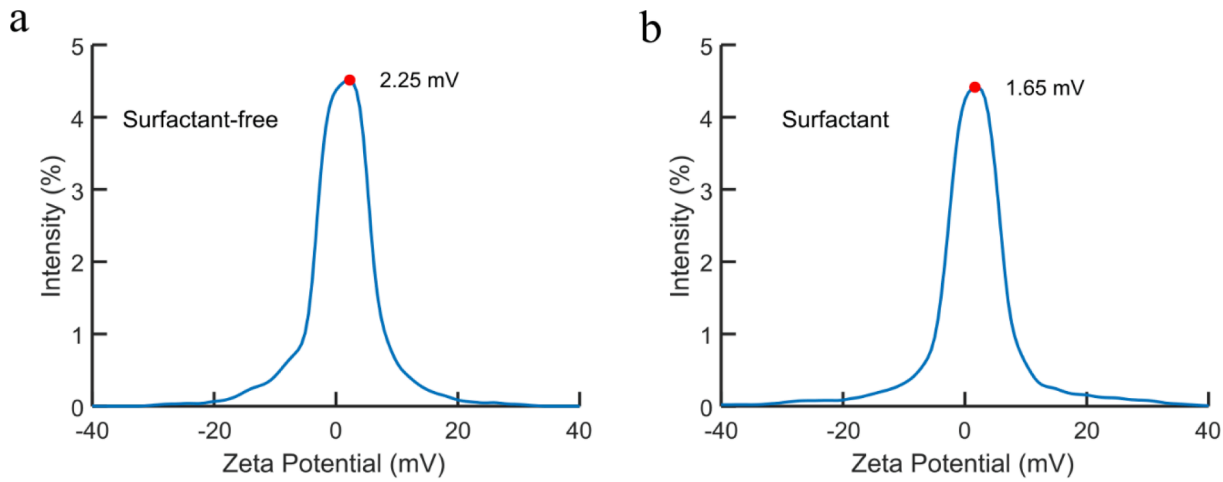

Fig. 7. Zeta potential of (a) surfactant-free and (b) surfactant curcumin oil emulsions. Peaks are labelled with a red dot with the related zeta potential written in. (For interpretation of the references to color in this figure legend, the reader is referred to the web version of this article.)

surface of the oil emulsions may protect oil droplets from coalescing, thereby contributing to the long-term stability observed in surfactant-free emulsions. It was noted that the large negative charge observed for emulsions in previous studies was mainly due to the presence of surface-active impurities. In our study we used filtered DI water, as well as filtering all other solutions before use which helps in limiting the presence of any impurities. This may help explain the near zero zeta potential measured in our study (Fig. 7).

An earlier study by Vácha *et al.* [29], which modelled a like system, came to similar conclusions as discussed in the previous paragraph. Using molecular dynamics, they observed a charge transfer occurring at the oil–water interfacial layer caused by the imbalance of donating and accepting hydrogen bonds of water molecules. This imbalance results in the generation of a partial charge. Subsequent experimental studies agreed with these findings. It was noted that lowering the pH of the solution, which increases the number of hydroxide ions, did not have an observable affect on the charge at the interface. This observation indicates that, when used in medicine, their electrostatic interactions with the environment will be similar no matter where they go, allowing for broader use.

Another possible factor that can affect the oil emulsion stability is the amount of saturated gas in the solution. Gas saturation in an aqueous solution has been shown to affect the stability of oil emulsions with the greatest stability found in degassed solutions [32–35]. A change in temperature can lead to a change in the amount of saturated gas. At low temperatures more gas can be stored in solution leading to oversaturation. When the sample starts to heat up during the measurement, bubbles can nucleate and be stabilized in the presence of a surfactant. These bubbles may start to interact with the water, oil, surfactant, and other bubbles in the solution resulting in a complicated network that affects our measurements. With increased storage time, the gas saturation changes leading to further changes in the sample. In surfactant-free samples the diffusion and dissolution of these gas bubbles will be quicker resulting in fewer interactions between the sample and the nucleated bubbles. Due to this, a bigger effect is expected to be observed for the surfactant containing samples and my help to explain the shifts seen in Fig. 6.

By extension Carpenter Cholakova *et al.* [36] noted that temperature variations spontaneously alter the shape of oil droplets. The constant change in concentration observed in Fig. 6d may, in part, be a side effect of droplet deformation due to the temperature difference between the storage area and the NanoSight. As the NanoSight settings detect circular particles only, any deformed droplets would be filtered out.

Lastly, the sample stability may also be affected by sample handling in the NanoSight. Not only does the machine consume the sample, but the mechanical pump that pushes the sample over the stage can lead to changes in particle size and concentration. These droplets may be squeezed intermittently so that collision and coalescence occur, thus affecting the emulsion size equilibrium. The surfactant samples in cold storage may be subjected to a bigger influence of these mechanical effects due to bubble formation detailed in section 3.5.

4.3. *Effects of a surfactant*

Surfactants are widely used in making emulsions due to their unique properties such as low surface tension in addition to their structural composition consisting of both hydrophobic and hydrophilic regions. The hydrophobic region has a high affinity to oil, the hydrophilic region on the other hand tends to dissolve in water. Surfactants therefore interlocate naturally between water and oil phases, helping to stabilize oil emulsions in water or water in oil emulsions. The lipophilic-hydrophobic balance (HLB) value determines how different surfactants are chosen for water in oil or oil in water emulsions. Usually, a surfactant with a high HLB value is used for oil in water emulsions. Herein, we choose SDS (HLB = 40) as a positive control to study the surfactant effect on oil in water emulsions.

The size of the emulsions in the surfactant-free and surfactant samples of do not change significantly. In comparison, the presence of a surfactant had an observed effect on the initial emulsion size, it being larger than the surfactant-free sample. In general, these changes are negligible in the context of the duration of the stability study. It should be noted that we are aware that, as the measurements are performed at room temperature the cold storage samples may have been affected by the temperature change during the measurements. However, the duration of these measurements was only a few minutes. When temperature increases, gas bubbles may form due to the decrease of gas solubility in water. As oil droplets are hydrophobic with a preference of attracting dissolved gas to the oil–water interface, this may facilitate a size increase of the nanoemulsions with time until an equilibrium has been reached. The presence of surfactant, such as SDS, imparts surface charges, which help to stabilize the newly nucleated bubbles. Nonetheless, all samples are still within the acceptable range of 200 nm or below for use in medicine. This is an optimal size range for use with the enhanced permeability and retention (EPR) effect where the large permeations in tissue surrounding cancer cells are taken advantage of for passive targeting [37,38].

In contrast, surfactant-free samples in this study show a better stability than samples stabilized by surfactant, particularly in cold storage. This unique property of our emulsion generation approach has many potential uses in pharma industry, as many medicines are required to be

kept in the fridge for better stability. In addition, the absence of a surfactant in our method, removes the negative side effects caused by surfactant traces, and, in addition, may increase the bioavailability of many drugs. Extended emulsion stability in cold storage would simultaneously extend the drug stability, and, as room temperature storage was also demonstrated to be relatively stable, surfactant-free emulsions may also positively impact medicine handling at room temperature.

4.4. Comparison with other generation methods

Generation of nanoemulsions without the use of surfactants is challenging as segregation of immiscible liquid consumes significant levels of energy [39]. This work provides a simple protocol for surfactant-free nanoemulsions, that is rapid, and easy to use. We compared the characteristics of emulsions made by a variety of traditional methods to demonstrate the merits of our current work, Fig. 8. The emulsion in the top right corner of the figure was generated by speed mixing without use of any surfactant, showing a high polydispersity.

When reviewing the different generation methods, it appears that the variation in size and polydispersity is not strictly reliant on generation method. Spontaneous emulsification appears to give the widest distribution with respect to both size and polydispersity. Garzoli et al. [17] generated nanoemulsions with different essential oils whose characteristics need to be taken into account when evaluating their data. In addition, the sample with the highest polydispersity did not contain an emulsifier which was used to improve the homogeneity of their resultant nanoemulsion. The outlier sample from Feng et al. [40] was an emulsion generated without the presence of a surfactant where the other samples contain varying combinations of Tween80 and lecithin. In general, the common methods applied for emulsion generation result in emulsions with sizes from 100 nm to 500 nm, but all of these experiments also apply surfactants and other chemicals to achieve these results.

When comparing the method of generation there is considerable overlap in the resulting size and polydispersity suggesting that the method of choice may not be the deciding factor. It should be noted however that a perfect comparison is not possible as experimental setup

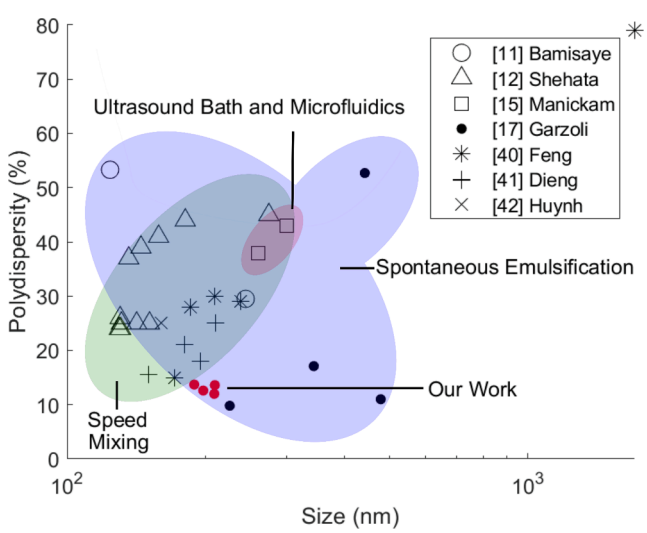

Fig. 8. Size and polydispersity comparison between oil emulsions in literature (black) and oil emulsions in this work (red). All data points, except [15], were taken from the text or tables provided in the cited papers. For [15] the data was read off a figure. To the best of our knowledge, all data included are taken from the time of generation for each emulsion. Colors represent similar methods used for emulsion generation. The outlier point at top right belongs to green shaded region. Blue: spontaneous emulsification, green: speed mixing, such as homogenizers, and red: ultrasound bath in combination with microfluidics. [11,12,15,17,40–42] (For interpretation of the references to color in this figure legend, the reader is referred to the web version of this article.)

and testing procedures vary from group to group. This is especially true for microfluidics where channel design plays a major role in the final product. Even when taking these factors into consideration it is still possible to conclude that complete control of the emulsion size cannot be achieved with current methods.

When comparing to the other authors, our Nanopore system was able to produce nanoemulsion of a specific size with a controlled polydispersity regardless of the presence of a surfactant as compared to Feng et al. and Garzoli et al. [17,40] discussed above. From the figure it is apparent that our Nanopore system can generate emulsions with similar characteristics of other research groups using a simpler method.

4.5. Future in biomedicine

The stability of oil emulsions generated in this study regardless of surfactant use indicates their usefulness in the drug delivery sector. Using oil emulsions for drug delivery not only increases the load efficiency due to the readiness of many drugs to dissolve in oil rather than aqueous solutions, but, as demonstrated here, it can contribute to the ease of generation. For initial testing, the cancer drug curcumin was dissolved in oil and thereby incorporated into the emulsions. Using UV–Vis we measured the initial concentration of curcumin in all four samples to be 0.52 μM. After a week the concentration was 0.51 μM. After a further week however the intensity of the measurements dropped off most likely due to fluorescence bleaching as the same aliquot was used for each measurement.

The encapsulation efficiency was calculated as the total amount of drug loaded in the sample, as measured by UV–Vis, divided by the total amount of drug added to the solution, here 50 μL for each emulsion sample. From this we measured the encapsulation efficiency for all samples to be around 7 %. This is a low efficiency and future work will investigate how to improve the encapsulation. In addition, it is important to test the curcumin before and after ultrasound treatment to ensure the emulsion generation process has no negative effects on its efficacy.

5. Conclusion

This paper investigated the generation of surfactant-free oil in water emulsions by using a nanopore membrane combined with ultrasound. It is a quick and simple method to produce oil emulsions. The emulsions generated with our approach are at physiological pH, and their stability was superior as demonstrated with DLS and NTA over the course of two weeks testing two different variables: storage temperature, and the presence or absence of a surfactant. This data presents stable emulsions where size and nanoemulsion concentration are independent of the presence of a surfactant. The storage temperature, as well as solution temperature at time of generation appeared to have a more significant effect on the nanoemulsions. To provide an example of their use we incorporated a known cancer drug, curcumin, into the oil. We found that the concentration of the incorporated curcumin was stable over several days. Overall, this study paves the way for new applications of oil nanoemulsion within the medical field.

CRediT authorship contribution statement

Helena H.W.B. Hansen: Writing – review & editing, Writing – original draft, Methodology, Investigation, Formal analysis, Data curation. **Gregor Kijanka:** Writing – review & editing, Data curation. **Lingxi Ouyang:** Writing – review & editing. **Nam-Trung Nguyen:** Supervision. **Hongjie An:** Writing – review & editing, Writing – original draft, Supervision, Project administration, Funding acquisition, Formal analysis, Conceptualization.

Declaration of competing interest

The authors declare that they have no known competing financial

interests or personal relationships that could have appeared to influence the work reported in this paper.

Data availability

The data that has been used is confidential.

Acknowledgement

H.A. gratefully acknowledges the funding support of the Australian Research Council though the ARC Future Fellowship (FT180100361) and ARC Discovery Project (DP230100556).

References

[1] S.N. Kale, S.L. Deore, Emulsion micro emulsion and nano emulsion: a review, Systematic Reviews in Pharmacy 8 (1) (2017) 39.
[2] R.J. Wilson, et al., Nanoemulsions for drug delivery, Particuology 64 (2022) 85–97.
[3] Y. Ozogul, et al., Recent developments in industrial applications of nanoemulsions, Adv. Colloid Interface Sci. 304 (2022) 102685.
[4] K. Sneha, A. Kumar, Nanoemulsions: techniques for the preparation and the recent advances in their food applications, Innov. Food Sci. Emerg. Technol. 76 (2022) 102914.
[5] I.F. Mustafa, M.Z. Hussein, Synthesis and technology of nanoemulsion-based pesticide formulation, Nanomaterials 10 (8) (2020) 1608.
[6] J.M.M. de Oca-Ávalos, R.J. Candal, M.L. Herrera, Nanoemulsions: stability and physical properties, Curr. Opin. Food Sci. 16 (2017) 1–6.
[7] R. Fopase, et al., Lipopeptide and essential oil based nanoemulsion for controlled drug delivery, Polymer-Plastics Technology and Materials 59 (18) (2020) 2076–2086.
[8] S. Sugumar, A. Mukherjee, N. Chandrasekaran, Eucalyptus oil nanoemulsion-impregnated chitosan film: antibacterial effects against a clinical pathogen, Staphylococcus aureus, in vitro, Int. J. Nanomed. 10 (sup2) (2015) 67–75.
[9] S.S. Silva, et al., Chitosan/Virgin-coconut-oil-based system enriched with cubosomes: a 3D drug-delivery approach, Mar. Drugs 21 (7) (2023) 394.
[10] C. Liu, et al., Development of low-oil emulsion gel by solidifying oil droplets: roles of internal beeswax concentration, Food Chem. 345 (2021) 128811.
[11] A. Bamisaye, et al., Fabrication, characterization, antimicrobial, toxicity and potential drug-delivery studies of PEGylated Sesamum indicum oil based nanoemulsion system, Beni-Suef University Journal of Basic and Applied Sciences 12 (1) (2023) 1–15.
[12] T.M. Shehata, et al., Myrrh essential oil-based nanolipid formulation for enhancement of the antihyperlipidemic effect of atorvastatin, J. Drug Delivery Sci. Technol. 61 (2021) 102277.
[13] M. Zhang, et al., A stable peony seed oil emulsion that enhances the stability, antioxidant activity, and bioaccessibility of curcumin, LWT 173 (2023) 114408.
[14] V.K. Maurya, M. Aggarwal, A phase inversion based nanoemulsion fabrication process to encapsulate vitamin D3 for food applications, J. Steroid Biochem. Mol. Biol. 190 (2019) 88–98.
[15] S. Manickam, K. Sivakumar, C.H. Pang, Investigations on the generation of oil-in-water (O/W) nanoemulsions through the combination of ultrasound and microchannel, Ultrason. Sonochem. 69 (2020) 105258.
[16] C.-X. Du, et al., Low-oil-phase emulsion gel with antioxidant properties prepared by soybean protein isolate and curcumin composite nanoparticles, LWT 161 (2022) 113346.
[17] S. Garzoli, et al., Lavandula x intermedia essential oil and hydrolate: evaluation of chemical composition and antibacterial activity before and after formulation in nanoemulsion, Ind. Crop. Prod. 145 (2020) 112068.
[18] X. Zhu, et al., Enhancing oil-in-water emulsion separation performance of polyvinyl alcohol hydrogel nanofibrous membrane by squeezing coalescence demulsification, J. Membr. Sci. 630 (2021) 119324.
[19] N.T.T. Uyen, Z.A.A. Hamid, N.B. Ahmad, Synthesis and characterization of curcumin loaded alginate microspheres for drug delivery, J. Drug Delivery Sci. Technol. 58 (2020) 101796.
[20] T.-L. Hwang, et al., Activated human neutrophil response to perfluorocarbon nanobubbles: oxygen-dependent and-independent cytotoxic responses, Toxicol. Lett. 203 (2) (2011) 172–180.
[21] T.-L. Pan, et al., Toxicological effects of cationic nanobubbles on the liver and kidneys: biomarkers for predicting the risk, Food Chem. Toxicol. 50 (11) (2012) 3892–3901.
[22] M.A. Motin, M.H. Mia, A.N. Islam, Thermodynamic properties of sodium dodecyl sulfate aqueous solutions with methanol, ethanol, n-propanol and iso-propanol at different temperatures, J. Saudi Chem. Soc. 19 (2) (2015) 172–180.
[23] S.-W. Ohl, et al., Creation of cavitation activity in a microfluidic device through acoustically driven capillary waves, Lab Chip 10 (14) (2010) 1848–1855.
[24] Q. Zeng, H. An, C.-D. Ohl, Wall shear stress from jetting cavitation bubbles: influence of the stand-off distance and liquid viscosity, J. Fluid Mech. 932 (2022) A14.
[25] P. Koukouvinis, et al., Parametric investigations of the induced shear stress by a laser-generated bubble, Langmuir 34 (22) (2018) 6428–6442.
[26] Botet, R. The“ ouzo effect”, recent developments and application to therapeutic drug carrying. in Journal of Physics: Conference Series. 2012. IOP Publishing.
[27] S. Pullanchery, S. Kulik, S. Roke, Water structure at the hydrophobic nanodroplet surface revealed by vibrational sum frequency scattering using isotopic dilution, J. Phys. Chem. B 126 (16) (2022) 3186–3192.
[28] S. Pullanchery, et al., Charge transfer across C-H··· O hydrogen bonds stabilizes oil droplets in water, Science 374 (6573) (2021) 1366–1370.
[29] R. Vácha, et al., The orientation and charge of water at the hydrophobic oil droplet–water interface, J. Am. Chem. Soc. 133 (26) (2011) 10204–10210.
[30] Leunissen, M.E., et al., Electrostatics at the oil–water interface, stability, and order in emulsions and colloids. Proceedings of the National Academy of Sciences, 2007. 104(8): p. 2585-2590.
[31] Carpenter, A.P., et al., Formation and surface-stabilizing contributions to bare nanoemulsions created with negligible surface charge. Proceedings of the National Academy of Sciences, 2019. 116(19): p. 9214-9219.
[32] C. Zhang, G. Zheng, C.M. Nichols, Micellar partitioning and its effects on Henry's law constants of chlorinated solvents in anionic and nonionic surfactant solutions, Environ. Sci. Tech. 40 (1) (2006) 208–214.
[33] T. Shimotori, W.A. Arnold, Measurement and estimation of Henry's law constants of chlorinated ethylenes in aqueous surfactant solutions, J. Chem. Eng. Data 48 (2) (2003) 253–261.
[34] L.M. Vane, E.L. Giroux, Henry's law constants and micellar partitioning of volatile organic compounds in surfactant solutions, J. Chem. Eng. Data 45 (1) (2000) 38–47.
[35] C. Yang, et al., Effects of surfactants and salt on Henry's constant of n-hexane, J. Hazard. Mater. 175 (1–3) (2010) 187–192.
[36] D. Cholakova, et al., Control of drop shape transformations in cooled emulsions, Adv. Colloid Interface Sci. 235 (2016) 90–107.
[37] J. Wu, The enhanced permeability and retention (EPR) effect: the significance of the concept and methods to enhance its application, Journal of Personalized Medicine 11 (8) (2021) 771.
[38] H.H. Hansen, et al., Nanobubble technologies: applications in therapy from molecular to cellular level, Biotechnol. Adv. (2022) 108091.
[39] Y. Singh, et al., Nanoemulsion: concepts, development and applications in drug delivery, J. Control. Release 252 (2017) 28–49.
[40] T. Feng, et al., Emulsion-based delivery systems for curcumin: encapsulation and interaction mechanism between debranched starch and curcumin, Int. J. Biol. Macromol. 161 (2020) 746–754.
[41] S.M. Dieng, et al., Pickering nano-emulsions stabilized by solid lipid nanoparticles as a temperature sensitive drug delivery system, Soft Matter 15 (40) (2019) 8164–8174.
[42] N.A.K. Huynh, et al., Development of softgel capsules containing cyclosporine a encapsulated pine essential oil based self-microemulsifying drug delivery system, J. Drug Delivery Sci. Technol. 68 (2022) 103115.